細胞の相互誘導での運動持続性への界面効果

松下勝義, 鎌本直也, 須藤麻希, 藤本仰一

阪大院理 生物

概要

我々は界面張力の相互誘導を行うモデル細胞の集団運動の持続性への効果を細胞のクラスターについて調べた. そのモデル細胞は比較的小さい界面張力下では持続的ランダムウォークを示した. 対照的に, 大きな張力ではその持続性は失われ細胞の集団回転運動が現れた.

Interface Effect on Persistence of Cellular Mutually Guiding

Katsuyoshi Matsushita, Naoya Kamamoto, Maki Sudo, and Koichi Fujimoto

Department of Biological Science, Graduate School of Science, Osaka University.

Abstract

In this study, we investigated the effects of interface tension on the persistence time of the collective movement of mutual guiding in a model cell cluster. The model cells based on the cellular Potts model reduce the persistence time of the collective movement as interface tension decreases. Finally, collective cell rotation appears for large values of interface tension.

1 Introduction

Eukaryotic cells collectively move through biological processes [1–3]. During these movements, cells guide their motion through their cellular contacts, such as leader guiding [4] and mutual guiding [5] mechanisms. These guidings lead to an order in the directions of motion. In contrast to the leader guiding, our simulation for mutual guiding showed that confluent cells in the periodic boundary condition exhibit long persistent time beyond an observation time scale in movements [5]. The result does not directly explain natural collective movements because the interface of the leading edges shown in Fig. 1(a) may reduce the persistence time. In natural systems, cells form finite-size clusters accompanying the interface. Thus, the movement reflects the interface of the leading edges, which affects the guiding efficiency. For instance, leader guiding promotes interface fingering, which affects the movement [6, 7].

We consider two mutually guiding cells on the leading edge of the cluster to intuitively estimate this effect of the interface tension. On the interface, we assume that the two cells, 1 and 2, contact each other and they have a receptor on the leading edge and ligand on the membrane, as shown in Fig. 1(b). The leading edge of cell 2 extends along the surface of cell 1 by exerting tension when the receptor recognizes the ligand. During the movement due to the guiding, the interface tension γ_{E} and the intercellular tension γ_{C} also affect the motion of the leading edge as shown in Fig. 1(c) through Young's law [8]. Assuming that the friction i proportional to the movement velocity v, it follows that

$$v \propto 2\left(\delta q + \gamma_E\right)\cos\theta - \gamma_C, \tag{1}$$

where δq is the guiding tension owing to mutual guiding [5, 9]. In this equation, we count both the tensions from cell 2 to cell 1 and cell 1 to cell 2. δ is the tension per receptor, q is the receptor concentration, and θ is the contact angle defined in the figure. This equation estimates that the interface tension affects the mutual guiding. This effect becomes complex in persistence because q is an active degree of freedom for cells with persistence [4, 5]. To elucidate this effect beyond this estimation, such as the dependence of the persistence time on γ_{E}, we should simulate the collective movement of the mutual guiding.

In this study, we theoretically investigate the effect of interface tension on the persistence time of the collective movement of a cell cluster. We used the cellular Potts model [10] by incorporating mutual guiding [5]. We observed a short persistent time [11, 12] for relatively small values of γ_E, in contrast to the long persistence time in the previous investigation. Additionally, we observed that the persistence of movement disappears with the motion transition to a collective rotation for large values of the interface tension.

2 Model

In this study, we focused on the surface tension of a cell cluster. One of the well-describable mod-

els for surface tension is the cellular Potts model, which reproduces cell sorting [13, 14] and adhesion-inducing developmental processes [15–18]. The model can reproduce the mutual guiding using cell–cell adhesion [5, 19]. This model considers the Potts state $m(\boldsymbol{r})$ at site $\boldsymbol{r}$ on a square lattice with linear size L and periodic boundary conditions. $m(\boldsymbol{r})$ takes 0 for the case without cells. In contrast, $m(\boldsymbol{r})$ takes a number in 1, 2 ... N, corresponding to the cell index. Here, N is the number of cells, and it is constant in this simulation for simplicity. Each domain of Potts state m expresses the cell shape for the mth cell. In this interpretation, the Monte Carlo simulation of this configuration expresses the dynamics of the cells.

The Monte Carlo simulation is based on the Boltzmann weight $w = \exp(-\beta\mathcal{H})$, where β is a parameter of cell motility. $\mathcal{H}$ is the Hamiltonian and it consists of three terms

$$\mathcal{H} = \mathcal{H}_{\rm S} + \mathcal{H}_{\rm V} + \mathcal{H}_{\rm G}. \tag{2}$$

The first term denotes the surface tension [10]

$$\mathcal{H}_{\rm S} = \gamma_{\rm C} \sum_{\boldsymbol{r}\boldsymbol{r}'} \eta_{m(\boldsymbol{r})m(\boldsymbol{r}')}\eta_{0m(\boldsymbol{r}')}\eta_{m(\boldsymbol{r})0} + \gamma_{\rm E} \sum_{\boldsymbol{r}\boldsymbol{r}'} \eta_{m(\boldsymbol{r})m(\boldsymbol{r}')} \left[\delta_{0m(\boldsymbol{r}')} + \delta_{m(\boldsymbol{r})0}\right]. \tag{3}$$

The summations of $\boldsymbol{r}\boldsymbol{r}'$ represent those over the nearest and next-nearest sites. The same symbol hereinafter is used in the same manner. $\gamma_{\rm C}$ and $\gamma_{\rm E}$ are the surface tensions. η_{nm} denotes $1-\delta_{nm}$, where δ_{nm} is the Kronecker's δ. Herein, we focused on the γ_E-dependence of movement persistence.

The second term in Eq. (2) is the volume constraint,

$$\mathcal{H}_{\rm V} = \kappa \sum_m (1 - \frac{\sum_{\boldsymbol{r}} \delta_{mm(\boldsymbol{r})}}{A})^2, \tag{4}$$

where κ and A denote the volume stiffness and the reference area of cells, respectively.

The third term in Eq. (2) expresses the mutual guiding

$$\mathcal{H}_{\rm G} = -\delta \sum_{\boldsymbol{r}\boldsymbol{r}'} \eta_{m(\boldsymbol{r})m(\boldsymbol{r}')}\eta_{0m(\boldsymbol{r}')}\eta_{m(\boldsymbol{r})0} \times \left[q_{\boldsymbol{r}}^{m(\boldsymbol{r})} + q_{\boldsymbol{r}'}^{m(\boldsymbol{r}')}\right]. \tag{5}$$

Here, the receptor concentration is given by $q_{\boldsymbol{r}}^{m} = 1+\boldsymbol{p}_{m(\boldsymbol{r})}\cdot\boldsymbol{e}_{m(\boldsymbol{r})}$, where $\boldsymbol{p}_m$ is a unit vector denoting the density gradient of receptor molecules, $\boldsymbol{e}_m(\boldsymbol{r})$ is a unit vector from $\boldsymbol{R}_m$ to $\boldsymbol{r}$ and $\boldsymbol{R}_m$ is the center of the mth cell. Additionally, the sensing occurs in the direction of $\boldsymbol{p}_m$, which represents the leading edge of cells. In this term, the receptor molecule reduces the surface tension by sensing with contacting cells. As a result, it aligns the moving direction

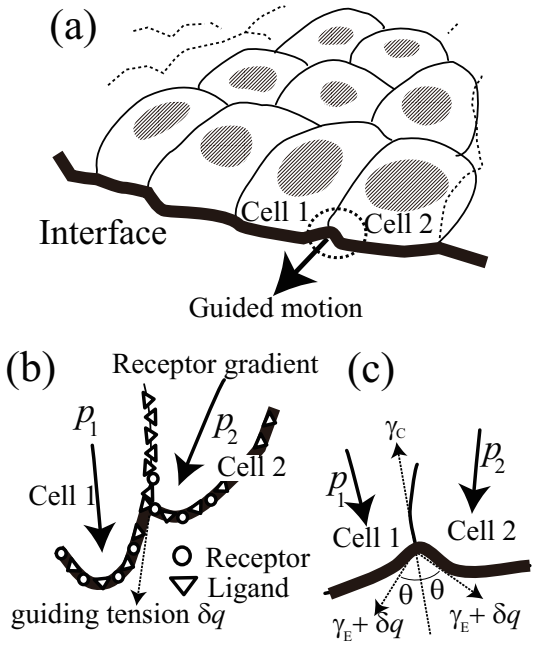

Fig. 1: (a) Cell cluster. (b) and (c) show the contact region of the leading edge between cells 1 and 2. (b) Motion guiding by cell 1 for cell 2 with their receptors and ligands. δq is the guiding tension, and $\boldsymbol{p}_m$ is the direction of the receptor concentration gradient of the mth cell. (c) Interface tensions. $\gamma_{\rm C}$ and $\gamma_{\rm E}$ denote the tension between cells and between cells and unoccupied space, respectively.

of the cell in the direction of the sensed cells. The derivation of this equation is based on [20, 21].

Here, we consider that sensing occurs at the leading edge of the cells. To express this situation, we assume that $\boldsymbol{p}_m$ obeys the equation of motion [22],

$$\frac{d\boldsymbol{p}_m}{dt} = \frac{1}{\tau}\left[\hat{I} - \boldsymbol{p}_m \otimes \boldsymbol{p}_m\right] \cdot \frac{d\boldsymbol{R}_m}{dt}, \tag{6}$$

where t, $\otimes$, $\hat{I}$, and τ denote the time, the tensor product, the unit tensor, and the time scale ratio of $d\boldsymbol{R}_m/dt$ to $d\boldsymbol{p}_m/dt$, respectively. The ratio determines the persistence of motion.

Based on $\mathcal{H}$, we consider the following conventional Monte Carlo simulations [10]: A single Monte Carlo step (MCS) consists of $16L^2$ copy trials, and it is the unit of time. In the copy trial, the state at the randomly chosen site, $\boldsymbol{r}$, changes to the state of a randomly chosen neighboring site. The copy is accepted with the Metropolis probability, $\min[1, w'/w]$, where w' is the Boltzmann weight with the state copy. $\boldsymbol{p}_m$ and $\boldsymbol{R}_m$ are constant in these copies and they change once after the single Monte Carlo step, by according to Eq. (6) and $\boldsymbol{R}_m = \sum_{\boldsymbol{r}} \boldsymbol{r}\delta_{mm(\boldsymbol{r})}/\sum_{\boldsymbol{r}}\delta_{mm(\boldsymbol{r})}$, respectively. The Euler method is used with a time difference of $1/\tau = 0.2$.

For the examination, we set $N = 64$, $A = 64$, κ

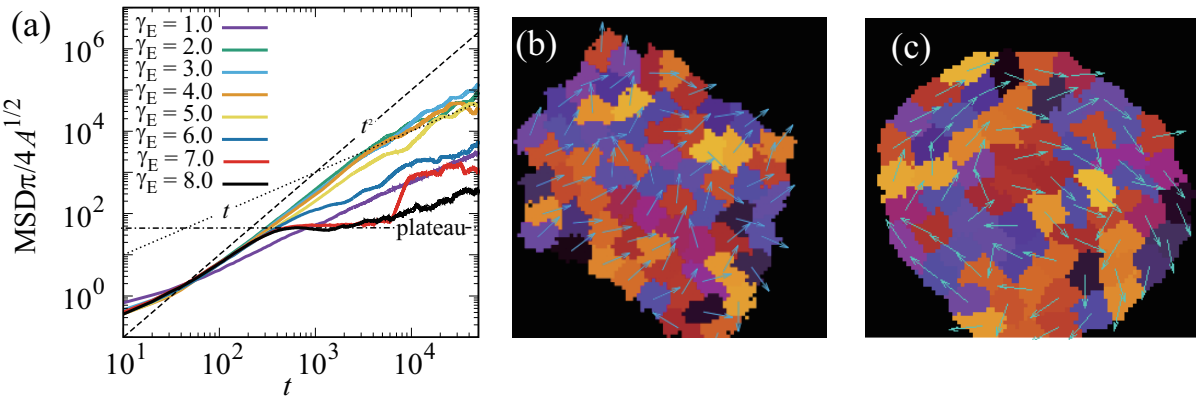

Fig. 2: (a) MSD as a function of t with γ_E sweeping. (b) Snapshot of cell configuration for $\gamma_E = 2.0$. (c) Snapshot of cell configuration for $\gamma_E = 7.0$. The black domain and other colored domains represent the unoccupied space and cells. The arrows from the center of the domains represent the $\boldsymbol{p}_m$ for each cell.

$= 64^2$, $\tau = 5.0$, $\delta = 0.5$ and $\beta = 0.2$ as empirically known parameters to observe the collective movement. We consider $\gamma_C = 2.5$ to choose the transition point between the dispersing state of cells and the aggregating state around the range of γ_E from 1.0 to 2.0. Here, the dispersing state is the state where the cells do not form contacts and separately take an individual random walk. To investigate the effect of interface tension, we consider γ_E from 1.0 to 8.0 and observe the collective motion.

3 Results

To investigate the persistence time of the collective cell movement, we calculated the mean square displacement of the cluster as a function of MCS t,

$$\mathrm{MSD}(t) = \left\langle \left[\int_{t_i}^{t+t_i} dt' \frac{1}{N} \sum \boldsymbol{d}_m(t') \right]^2 \right\rangle. \quad (7)$$

Here, we relax the state during t_0 MCS and then calculate MSD from $t = t_i$ to $t = t_f$. We take $t_i = 10^4$ MCS and $t_f = 5 \times 10^4$ MCS. $\boldsymbol{d}_m$ is the displacement of the mth cell for 1 MCS. The angle bracket $\langle \dots \rangle$ represents the average of the eight trajectories. The MSDs for various γ_E values are plotted in Fig. 2(a), where the diameter of the cells, $2\sqrt{A/\pi}$, is unity. At $\gamma_E = 1.0$, the cells were in a dispersing state. In this case, the MSD is proportional to the number of MCS t in the data. This behavior reflects individual random walks of cells.

For $\gamma_E \geq 2.0$, the cells take an aggregating state. At $\gamma_E = 2.0$, MSD behaves in the superdiffusive motion like a ballistic motion with MSD $\simeq t^2$ up to $t \sim 10^3$ MCS and then crossover to a random walk as MSD $\sim t$. The ballistic motion in a short time originates from the memory effect in Eq. (6) [5]. This behavior is the same up to $\gamma_E = 6.0$. For these data, the long persistence time previously observed is absent. This result indicates that the interface of the leading edges reduces the persistence time.

A distinctive observation is that the time scale of the superdiffusive motion steadily decreased with γ_E from 6.0. Additionally, a subdiffusive plateau was observed in MSD for $\gamma_E \simeq 7.0$ in an intermediate time scale longer than that of the ballistic motion, like glassy liquid systems [23]. For $\gamma_E > 7.0$, the subdiffusive plateau also appears. This result indicates that a large interface tension suppresses the persistence time.

To elucidate this suppression, snapshots for $\gamma_E = 2.0$ and $\gamma_E = 7.0$ are shown in Fig. 2(b) and (c), respectively. The configurations of the arrows of $\boldsymbol{p}_m$ largely differ in these snapshots. For $\gamma_E = 2.0$, $\boldsymbol{p}_m$ exhibits an ordered state and drives collective cell movement. In contrast, $\boldsymbol{p}_m$ for $\gamma_E = 7.0$ forms a vortex and drives a rotational motion similar to that of *Dictyostelium discoideum* in the mound stage [24]. The rotation direction exhibits persistence for large γ_E in our observation time and merely changes at $\gamma_E = 7.0$ through stochastic transitions between a translational motion to the rotation, which is the origin of sudden changes in MSD in Fig. 2(a) The emergence of this rotational motion is an origin that suppresse the persistence of the collective cell movement.

4 Summary and Discussions

We investigated the effect of the interface tension of the leading edges of cell clusters on the persistence time of collective movement. The interface tension reduces the long persistence time previously that was observed even for relatively small interface tensions [5]. In contrast, the large interface tension inhibits the persistence. This suppression originates from the emergence of rotational motion.

Additionally, long-timescale persistence appears for excluding volume-interacting cells with periodic boundary and confluent conditions [25–27]. Therefore, the corresponding systems with the interface may change the results. However, these works as-

sume the repulsion in contrast to the case with mutual guiding; hence cannot realize the cell cluster. Therefore, another method that incorporates an interface is necessary for the examination.

Finally, we consider the emergence of rotational motion for a large interface tension. In our simulation, a large interface tension resulted in a large θ. Here, large θs' values of near $\pi/2$ correspond to the smooth interface shown in Fig. 2(c). The smooth interface aligns the force from tensions γ_E and δq in the tangential direction at the interface. Therefore, the guiding of δq induces torque on the interface around the center of the cell cluster. As a result, it leads to collective rotation.

Notably, this mechanism of rotation differs from those of already known cell rotations, which originate from chemotaxis [28, 29], flocking interactions [30], anisotropic apical constriction [31], contact following [32, 33], and minority control effect of leader cells [34]. The mechanism through mutual guiding is one of the collective rotations unknown so far in the sense that cells make good use of the surface tension.

We thank S. Yabunaka, H. Kuwayama, H. Hashimura, M. Sawada, and K. Sawamoto for providing various relative knowledge. We also thank M. Kikuchi and H. Yoshino for their support with the research resource. This work was supported by JSPS KAKENHI (Grant Number 19K03770) and by AMED (Grant Number JP19gm1210007).

References

[1] C. J. Weijer, J. Cell Sci. **122**, 3215 (2015).

[2] P. Friedl and D. Gilmour, Nat. Rev. Mol. Cell Biol. **10**, 445 (2009).

[3] P. Rørth, Annu. Rev. Cell Dev. Biol. **25**, 407 (2009).

[4] A. J. Kabla, J. R. Soc. Interface **9**, 3268 (2012).

[5] K. Matsushita, Phys. Rev. E **97**, 042413 (2018).

[6] M. Poujade, E. Grasland-Mongrain, A. Hertzog, J. Jouanneau, P. Chavrier, B. Ladoux, A. Buguin, and P. Silberzan, Proc. Natl. Acad. Sci. USA **104**, 15988 (2007).

[7] S. Mark, R. Shlomovitz, N. S. Gov, M. Poujade, E. Grasland-Mongrain, and P. Silberzan, Biophys. J. (2010).

[8] P.-G. de Gennes, F. Brochard-Wyart, and D. Quere, *Capillarity and Wetting Phenomena: Drops, Bubbles, Pearls, Waves* (Springer, 2004).

[9] S. Okuda and K. Sato, arXiv:2104.13059 (2021).

[10] F. Graner and J. A. Glazier, Phys. Rev. Lett. **69**, 2013 (1992).

[11] L. Li, S. F. Nørrelykke, and E. C. Cox, PLoS One **3**, e2093 (2008).

[12] H. Takagi, M. J. Sato, T. Yanagida, and M. Ueda, PLoS One **3**, e2648 (2008).

[13] F. Graner, J. Theor. Biol. **164**, 455 (1993).

[14] J. A. Glazier and F. Graner, Phys. Rev. E **47**, 2128 (1993).

[15] A. F. M. Marée and P. Hogeweg, Proc. Natl. Am. Sci. USA **98**, 3879 (2001).

[16] A. R. A. Anderson, M. A. J. Chaplain, and K. A. Rejniak, *Single-Cell-Based Models in Biology and Medicine* (Birkhauser Verlag AG, Basel, 2007).

[17] M. Scianna and L. Preziosi, *Cellular Potts Model* (CRC Press, UK, 2013).

[18] T. Hirashima, E. G. Rens, and R. M. H. Merks, Dev. Growth Differ. **59**, 329 (2017).

[19] K. Matsushita, Phys. Rev. E. **95**, 032415 (2017).

[20] K. Matsushita, Phys. Rev. E **101**, 052410 (2020).

[21] K. Matsushita, H. Hashimura, H. Kuwayama, and K. Fujimoto, arxiv:2110.00235 (2021).

[22] B. Szabó, G. J. Szollosi, B. Gonci, Z. Juranyi, D. Selmeczi, and T. Vicsek, Phys. Rev. E **74**, 061908 (2006).

[23] R. Yamamoto and A. Onuki, Phys. Rev. E **58**, 3515 (1998).

[24] J. T. Bonner, *The Social Amoebae: The Biology of Cellular Slime Molds* (Princeton University Press, Princeton, 2009).

[25] K. Matsushita, K. Horibe, N. Kamamoto, and K. Fujimoto, J. Phys. Soc. Jpn. **88**, 103801 (2019).

[26] K. Matsushita, K. Horibe, N. Kamamoto, S. Yabunaka, and K. Fujimoto, Proc. Sympo. Traffic Flow Self-driven Particles **25**, 21 (2019).

[27] K. Matsushita, S. Yabunaka, and K. Fujimoto, J. Phys. Soc. Jpn. **90**, 054801 (2020).

[28] F. Siegert and C. J. Weijer, Curr. Biol. **5**, 937.

[29] B. Vasiev, F. Siegert, and C. J. Weller II, J. Theor. Biol. **184**, 441 (1997).

[30] W.-J. Rappel, A. Nicol, A. Sarkissian, H. Levine, and W. F. Loomis, Phys. Rev. Lett. **83**, 1247 (1999).

[31] K. Sato, T. Hiraiwa, E. Maekawa, A. Isomura, T. Shibata, and E. Kuranaga, Nat. Commun. **6**, 10074 (2015).

[32] T. Umeda and K. Inouye, J. Theor. Biol. **219**, 301 (2002).

[33] T. Hiraiwa, Phys. Rev. Lett. **125**, 268104 (2020).

[34] K. Matsushita, S. Yabunaka, H. Hashimura, H. Kuwayama, and K. Fujimoto, Proc. Sympo. Traffic Flow Self-Driven Parti. **26**, 38 (2020).

E-mail: kmatsu@bio.sci.osaka-u.ac.jp

Erratum: 細胞の相互誘導での運動持続性への界面効果

松下勝義, 鎌本直也, 須藤麻希, 藤本仰一

阪大院理 生物

Erratum: Interface Effect on Persistence of Cellular Mutually Guiding

Katsuyoshi Matsushita, Naoya Kamamoto, Maki Sudo, and Koichi Fujimoto

Department of Biological Science, Graduate School of Science, Osaka University.

In the paper[1], equation (1) and Fig. 1 are inconsistent with Eq. (5). Because Eq. (5) is correct as the mutual guiding [2, 3], Equation (1) and symbols in Fig. (1) should change as listed in Table 1. The paper is based only on Eq. (5). Hence, the results and conclusions in the paper are correct.

Table 1: lists of corrections

	Error	Correction
Eq. (1)	$v \propto 2\,(\gamma_E + \delta q)\cos\theta - \gamma_C$	$v \propto 2\gamma_E \cos\theta - (\gamma_C - 2\delta q)$
In Fig. (1)	$\gamma_E + \delta q$	γ_E
In Fig. (1)	γ_C	$\gamma_C - 2\delta q$

References

[1] K. Matsushita, N. Kamamoto, M. Sudo, and K. Fujimoto, Proceedings of the Symposium on Traffic Flow and Self-Driven Particles **27**, 23 (2021).

[2] K. Matsushita, Phys. Rev. E **97**, 042413 (2018).

[3] K. Matsushita, Phys. Rev. E **101**, 052410 (2020).

E-mail: kmatsu@bio.sci.osaka-u.ac.jp